

DO-TH-98/19

The nucleon in the chiral quark model: an alternative computation scheme

Jürgen Baacke* and Hendrik Sprenger†

Institut für Physik, Universität Dortmund
D - 44221 Dortmund, Germany

Abstract

We formulate the quark sea contributions to the energy and various physical observables in terms of Euclidean Green functions and their K-spin partial wave reduction. In this framework it is not necessary to discretize the continuous spectrum by introducing a finite boundary. Using this formulation we perform a new self-consistent computation of the nucleon state in the Nambu-Jona-Lasinio model. Besides this technical advantage such an alternative computation scheme makes it possible to obtain the numerical predictions of the model in an entirely independent way. We use the Pauli-Villars cutoff to define the model. Our results for the nucleon energy, the mesonic profile, and various observables essentially confirm results obtained by other groups using this regularization. The results for g_A , obtained on the basis of quark currents, are close to the experimental value.

Keywords:

non-perturbative methods, effective chiral models, chiral solitons, models of baryons

PACS:

12.38.Lg, 12.39.-x, 12.39.Fe, 12.40.Yx

*Email address: baacke@physik.uni-dortmund.de

†Email address: sprenger@hal1.physik.uni-dortmund.de

1 Introduction

The Nambu-Jona-Lasinio (NJL) model [1] has received a wide attention during the last decade [3], following previous attempts [5, 6] to describe the nucleon in the large- N_c limit on the basis of mesonic degrees of freedom. In the NJL model, the mesons appear as effective degrees of freedom, parametrizing condensates of the basic fermion fields. The basic model is a quark model with a four-fermion interaction, and therefore nonrenormalizable. The ultraviolet divergences are handled by introducing a cutoff which stays finite. Its functional form and numerical value, therefore, are relevant for the predictions of the model. Various cutoffs have been introduced, a good review of the different possibilities and their numerical impacts is given in [7]. Previously, the Schwinger proper-time cutoff was used almost exclusively until it was found [8] that this regularization violates the momentum sum rule for the parton distributions, and that Pauli-Villars regularization is favored in this respect.

The use of the Pauli-Villars regularization opens the possibility to introduce a technique for computing the effective action which has been developed previously [9, 11] and has been applied to a wide range of physical problems involving fluctuation determinants [12, 13]. It is based on using the Euclidean Green functions instead of summation of levels. Computing functional determinants and other expectation values involving the quark continuum by summing over levels and Minkowski space wave functions requires the introduction of space boundaries in order to discretize the spectrum. The associated space cutoff has to be removed, introducing a numerical limiting procedure. This limiting procedure seems to be technically well under control, as can be seen, e.g., by comparing computations of the sphaleron determinant using level summation [14] and Green function [12] techniques. Nevertheless, level summation is certainly not a very economical technique. Another way of encompassing the discretization of the spectrum has been proposed by Moussallam [17], who uses Minkowski space phase shifts. At the same time an alternative technique presents the possibility to obtain the predictions of the model in an independent way.

There are various methods to perform self-consistent computations [18]. As the equation of motion for the meson profiles requires to solve the equation of motion for the meson field, or, equivalently, the chiral angle, it is advantageous to be able to compute the functional derivative of the effective action with respect to the meson field. A technique for computing such derivatives using Euclidean Green functions has been set up recently [20] and used for a self-consistent computation of the bubble nucleation rate in the electroweak theory [21]. It is the purpose of this work to transfer these techniques, *mutatis mutandis*, to the NJL model. Apart from the self-consistent computation of the mesonic profiles of the nucleon we also formulate the sea quark contributions to various other observables, such as the moment of inertia, in terms of Euclidean Green functions. This latter aspect of our work is of course important; without it, one would have to go back to level summation in computing these observables and our technique would loose much of its attractiveness.

The NJL model, as considered here, is not a unique theory; there are many versions of it, the most elaborate ones [22] include the ρ , a_1 and ω vector mesons as well, as it was done before in the Skyrme model [24, 26]. However, even within the restricted class of models in which only the $\pi - \sigma$ fields are taken into account, there is a wide variety. These

models differ by the kind of regularization, as mentioned above, but also by applying it to various parts of the spectrum. In a renormalizable theory one would apply it only to the lowest perturbative contributions; in the NJL model it is applied to the finite parts as well. Furthermore, it was usually only applied to the quark sea, and not to the valence contribution. Some models also differ by the way in which the meson degrees of freedom are varied: the variation can be extended to both σ and π fields, or be restricted to the “chiral circle”, the 4-sphere being defined by $\sigma^2 + \pi^2 = f_\pi^2$. Unfortunately, the existence of nucleon solutions is not a robust property of the theory, such solutions are found only within a small subset of the different versions, a situation that must be considered as unsatisfactory. We will not add to the ongoing discussion (see e.g. [28]), we will use that version of the model recently used by Pobylitsa *et al.* [29] for computing the parton distributions. It only takes into account the π and σ fields, which are varied on the chiral circle only, and Pauli-Villars regularization is applied to the quark sea, not to the filled bound state.

2 The model

Starting with the NJL-Lagrangian [1]

$$\mathcal{L}_{\text{NJL}} = \bar{\psi}(i\gamma^\mu\partial_\mu - m)\psi + \frac{G}{2} [(\bar{\psi}\psi)^2 + (\bar{\psi}i\gamma_5\boldsymbol{\tau}\psi)^2] \quad (2.1)$$

one obtains after the standard bosonization procedure

$$S_{\text{NJL}} = \int d^4x \left\{ \bar{\psi} \left[i\gamma^\mu\partial_\mu - g(\sigma + i\boldsymbol{\pi} \cdot \boldsymbol{\tau}\gamma_5) \right] \psi - \frac{\mu^2}{2} (\sigma^2 + \boldsymbol{\pi}^2) + \frac{m\mu^2}{g} \sigma \right\}. \quad (2.2)$$

The parameters of the model are the fermion self-coupling G , the quark mass m , and the cutoff scale Λ . In the bosonized version these parameters appear as the quark-meson coupling g and the symmetry breaking mass parameter μ . They are related to the basic parameters as $g = \mu\sqrt{G}$ and $m\mu^2 = gf_\pi m_\pi^2$. The latter equation expresses μ in terms of physical constants and of the coupling g which remains a free parameter. A further relation is obtained from the gradient expansion of the effective action. The resulting kinetic term of the pion field is normalized correctly if the Pauli-Villars cutoff is fixed as

$$\Lambda = m_0 \sqrt{\exp\left(\frac{4\pi^2}{N_c g^2}\right)}. \quad (2.3)$$

If the $\sigma - \pi$ field is varied only on the chiral circle, the second term in Eq. (2.2) is absent. For static pion fields the action is proportional to the time τ ; the two remaining parts of the effective action then contribute to the energy as

$$E_{\text{fer}} = \frac{1}{\tau} \text{Tr} \log \left[-i\gamma^\mu\partial_\mu + \mathbf{m}(\mathbf{x}) \right], \quad (2.4)$$

$$E_{\text{br}} = -m_\pi^2 f_\pi \int d^3x (\sigma - f_\pi). \quad (2.5)$$

Here the trace is taken over the quark sea and - in the case of baryons - over the filled bound states. $\mathbf{m}(\mathbf{x})$ is given - on the chiral circle - by

$$\begin{aligned}\mathbf{m}(\mathbf{x}) &= g[\sigma + i\gamma_5 \boldsymbol{\tau} \cdot \boldsymbol{\pi}] \\ &= m_0[\exp\{i\gamma_5 \boldsymbol{\tau} \cdot \boldsymbol{\phi}(\mathbf{x})\}] \\ &= m_0[\cos(|\boldsymbol{\phi}(\mathbf{x})|) + i\gamma_5 \boldsymbol{\tau} \cdot \hat{\boldsymbol{\phi}}(\mathbf{x}) \sin(|\boldsymbol{\phi}(\mathbf{x})|)],\end{aligned}\quad (2.6)$$

where we have introduced the “dynamical quark mass” $m_0 = gf_\pi$. With the hedgehog ansatz $\boldsymbol{\phi}(\mathbf{x}) = \hat{\mathbf{x}}\vartheta(r)$ the mass becomes

$$\mathbf{m}(\mathbf{x}) = m_0[\cos(\vartheta(r)) + i\gamma_5 \boldsymbol{\tau} \cdot \hat{\mathbf{x}} \sin(\vartheta(r))]. \quad (2.7)$$

3 Basic relations

Given the profile $\vartheta(r)$, the energy of the corresponding nucleon state consists of the symmetry breaking part that can be evaluated trivially, and the contributions of valence and sea quarks. In order to evaluate the valence quark contribution we have to find the bound state energy by solving, with appropriate boundary conditions, the Dirac equation

$$(i\nu - H)\psi_0(\mathbf{x}) = 0. \quad (3.1)$$

Here we have introduced the Dirac Hamiltonian

$$H = -i\boldsymbol{\alpha} \cdot \boldsymbol{\nabla} + \gamma_0 \mathbf{m}(\mathbf{x}). \quad (3.2)$$

The computation of the quark sea contribution is more involved. We will recall here a method introduced previously [9, 11] in which the computation of the zero point energy is related to the Euclidean Green function

$$S_E(\mathbf{x}, \mathbf{x}', \nu) = \sum_{\alpha} \frac{\psi_{\alpha}(\mathbf{x})\psi_{\alpha}^{\dagger}(\mathbf{x}')}{-i\nu + E_{\alpha}}. \quad (3.3)$$

The subscript α is a formal notation for the discrete and continuum eigenstates of the Dirac Hamiltonian H ; we also indicate the positive energy eigenstates by $\alpha > 0$, the negative ones by $\alpha < 0$, and the valence eigenstate with $\alpha = 0$. S_E satisfies the equation

$$(i\nu - H)S_E(\mathbf{x}, \mathbf{x}', \nu) = -\delta^3(\mathbf{x} - \mathbf{x}'). \quad (3.4)$$

The zero point energy

$$E_{\text{sea}} = \sum_{\alpha < 0} E_{\alpha} \quad (3.5)$$

can be computed as a contour integral around the positive imaginary axis in the complex ν -plane, see Fig. 1, as

$$E_{\text{sea}} = \int_{C_-} \frac{d\nu}{2\pi i} \nu \text{Tr} \int d^3x S_E(\mathbf{x}, \mathbf{x}, \nu). \quad (3.6)$$

Deforming the contour to run along the real ν axis, and subtracting the zero point energy of the free Dirac operator $H_0 = -i\boldsymbol{\alpha} \cdot \boldsymbol{\nabla} + \gamma_0 m_0$, the integral takes the form

$$E_{\text{sea}} = -i \int_{-\infty}^{\infty} \frac{d\nu}{2\pi} \nu \text{Tr} \int d^3x [S_{\text{E}}(\mathbf{x}, \mathbf{x}, \nu) - S_{\text{E},0}(\mathbf{x}, \mathbf{x}, \nu)] . \quad (3.7)$$

The bound state can be included by deforming the contour to the one presented in Fig. 1 as a dashed line, however, we will consider the bound state separately here and below. It is convenient to introduce the bosonic Green function G_{E} via

$$S_{\text{E}} = (i\nu + H)G_{\text{E}} \quad (3.8)$$

which satisfies

$$(\nu^2 + H^2) G_{\text{E}}(\mathbf{x}, \mathbf{x}', \nu) = [\nu^2 - \Delta + m_0^2 + \mathcal{V}(\mathbf{x})] G_{\text{E}}(\mathbf{x}, \mathbf{x}', \nu) = \delta^3(\mathbf{x} - \mathbf{x}') \quad (3.9)$$

with the potential or vertex operator

$$\mathcal{V}(\mathbf{x}) = i\boldsymbol{\gamma} \cdot \boldsymbol{\nabla} \mathbf{m}(\mathbf{x}) . \quad (3.10)$$

In terms of G_{E} the energy can be written as

$$E_0 = \int_0^{\infty} \frac{d\nu}{\pi} \nu^2 \int d^3x \text{Tr} [G_{\text{E}}(\mathbf{x}, \mathbf{x}, \nu) - G_{\text{E},0}(\mathbf{x}, \mathbf{x}, \nu)] . \quad (3.11)$$

The expressions for the zero point energy and the subsequent manipulations are formal. Even after subtracting the free zero point energy, they only make sense if properly regularized. In order to understand the divergences of the subtracted zero point energy we use the resolvent expansion of the Green function with respect to the potential \mathcal{V} ; if it is inserted into the expression for the zero point energy we obtain

$$E_0 = \sum_{n=1}^{\infty} \frac{(-1)^n}{2n} \text{Tr} \int \frac{d\nu}{2\pi} \int \prod_{i=1}^n d^3x_i G_{\text{E},0}(\mathbf{x}_i - \mathbf{x}_{i-1}, \nu) \mathcal{V}(\mathbf{x}_i) \quad (3.12)$$

with $x_n = x_0$. We have subtracted the free zero point energy by omitting the zeroth order in the sum over n . The first order term vanishes after taking the trace, and the only divergent term is the second order one. Explicitly, it takes the form

$$E_0^{(2)} = \frac{1}{4} \int \frac{d^3q}{(2\pi)^3} \text{Tr} \tilde{\mathcal{V}}(\mathbf{q}) \tilde{\mathcal{V}}(-\mathbf{q}) \int_0^1 dx \int \frac{d^4p}{(2\pi)^4} \frac{1}{[p^2 + m_0^2 + q^2 x(1-x)]^2} , \quad (3.13)$$

where $\tilde{\mathcal{V}}(\mathbf{q})$ is the Fourier transform of the potential. The logarithmically divergent integral can be defined by using, below the integrand, the Pauli-Villars subtraction

$$E_0^{(2)} = \frac{1}{4} \int \frac{d^3q}{(2\pi)^3} \text{Tr} \tilde{\mathcal{V}}(\mathbf{q}) \tilde{\mathcal{V}}(-\mathbf{q}) \int_0^1 dx \frac{1}{16\pi^2} \left\{ \ln \Lambda^2 - \ln [m_0^2 + q^2 x(1-x)] \right\} . \quad (3.14)$$

Unlike in the case of renormalized perturbation theory here the regularization will be extended over the finite contributions as well, so that the regularized zero point energy reads

$$E_{0,\text{reg}} = E_0(m_0) - \frac{m_0^2}{\Lambda^2} E_0(\Lambda) , \quad (3.15)$$

where the subtraction is to be understood to be done below the \mathbf{x} and ν integrals, respectively (see below), before the partial wave summation and ν integration. The factor m_0^2/Λ^2 takes into account that the potential $\tilde{\mathcal{V}}(\mathbf{q})$ contains a factor m_0 , and a factor Λ in the subtracted part. These prefactors have to be compensated in order to ensure the cancellation of the divergent integrals.

The perturbative expansion, Eq. (3.12), can be used [20] to obtain an expression for the derivative of the zero point energy

$$\begin{aligned} \frac{\delta E_0}{\delta \phi_a(\mathbf{z})} &= \sum_{n=1}^{\infty} \frac{(-1)^n}{2} \int \frac{d\nu}{2\pi} \text{tr} \int d^3x_1 \frac{\delta \mathcal{V}(\mathbf{x}_1)}{\delta \phi_a(\mathbf{z})} \\ &\quad \times \int \left(\prod_{i=2}^n d^3x_i G_{E,0}(\mathbf{x}_i - \mathbf{x}_{i-1}, \nu) \mathcal{V}(\mathbf{x}_i) \right) G_{E,0}(\mathbf{x}_1 - \mathbf{x}_n, \nu) . \end{aligned} \quad (3.16)$$

The perturbative sum can be recollected into the full nonperturbative Green function, so that

$$\frac{\delta \overline{E_0^{(2)}}}{\delta \phi_a(\mathbf{z})} = \text{tr} \sum_{K,P} \int d^3x \frac{\delta \mathcal{V}(\mathbf{x})}{\delta \phi_a(\mathbf{z})} \int_0^\infty \frac{d\nu}{2\pi} \overline{G_E^{(1)}(\mathbf{x}, \mathbf{x}, \nu)} . \quad (3.17)$$

Here and in the following we use superscripts (j) to indicate that the expression is of order j in the potential \mathcal{V} , or its derivative. The symbol $\overline{(j)}$ indicates that the expression is evaluated to all orders in the potential starting with order j . So the exact zero point energy, after subtracting the zeroth order, and taking account of the vanishing of the first order, is of order $\overline{(2)}$, as indicated on the l.h.s. of the last equation. $\overline{G_E^{(1)}}$ on the r.h.s. includes all orders but the zeroth one. It remains to evaluate the derivative of $\mathcal{V}(\mathbf{x})$ with respect to ϕ_a . One obtains

$$\begin{aligned} \frac{\delta \mathcal{V}(\mathbf{x})}{\delta \phi_a(\mathbf{z})} &= im_0 \boldsymbol{\gamma} \cdot \boldsymbol{\nabla}_x \delta^3(\mathbf{x} - \mathbf{z}) \left[i\gamma_5 \tau_a \exp(i\gamma_5 \boldsymbol{\tau} \cdot \boldsymbol{\phi}(\mathbf{x})) \right. \\ &\quad \left. + i\gamma_5 (\tau_a - \phi_a(\mathbf{x}) \boldsymbol{\tau} \cdot \hat{\boldsymbol{\phi}}(\mathbf{x})) \frac{\sin |\boldsymbol{\phi}(\mathbf{x})|}{|\boldsymbol{\phi}(\mathbf{x})|} \right] . \end{aligned} \quad (3.18)$$

Inserting the hedgehog ansatz, $\boldsymbol{\phi}(\mathbf{x}) = \hat{\mathbf{x}}\vartheta(r)$ and using the fact that within the trace the expectation value of $\boldsymbol{\tau}$ must be parallel to $\hat{\boldsymbol{\phi}}$, i.e., $\tau_a \rightarrow \hat{x}_a \boldsymbol{\tau} \cdot \hat{\mathbf{x}}$, the derivative of the zero point energy takes the form

$$\begin{aligned} \left. \frac{\delta \overline{E_0^{(2)}}}{\delta \phi_a(\mathbf{z})} \right|_{\hat{\boldsymbol{\phi}}(\mathbf{x})=\hat{\mathbf{z}}\vartheta(r)} &= -m_0 \text{tr} \gamma_5 \tau_a [\cos(\vartheta(r)) - i\gamma_5 \boldsymbol{\tau} \cdot \hat{\mathbf{z}} \sin(\vartheta(r))] \\ &\quad \times \int_0^\infty \frac{d\nu}{2\pi} \boldsymbol{\gamma} \cdot \boldsymbol{\nabla}_z \overline{G_E^{(1)}}(\mathbf{z}, \mathbf{z}, \nu) . \end{aligned} \quad (3.19)$$

The gradient acts on the Green function at equal arguments. It is taken after carrying out that limit. The Euclidean Green function can be expanded [30] with respect to K-spin harmonics Ξ_n^{K,K_z} (for details see Appendix A) as

$$G_E(\mathbf{z}, \mathbf{z}', \nu) = \sum_{K, K_z, P} g_{mn}^{K, P}(r, r', \nu) \Xi_m^{K, K_z}(\hat{\mathbf{z}}) \otimes \Xi_n^{K, K_z \dagger}(\hat{\mathbf{z}}') . \quad (3.20)$$

The radial Green functions form 4×4 matrices; they can be written in terms of mode functions³ $f_n^{\alpha+}(r)$ and $f_n^{\alpha-}(r)$ which are solutions regular at $r = 0$ and as $r \rightarrow \infty$, respectively, of a system of radial differential equations given in Appendix A. Explicitly, they are given by

$$g_{mn}(r, r') = \kappa \left[\theta(r - r') f_m^{\alpha+}(r) f_n^{\alpha-}(r') + \theta(r' - r) f_m^{\alpha-}(r) f_n^{\alpha+}(r') \right] . \quad (3.21)$$

The superscript α labels 4 linearly independent solutions.

In this basis, and using the reduced Green functions, the zero point energy takes the form [11]

$$E_0^{(2)} = N_c \int_0^\infty \frac{d\nu}{\pi} \nu^2 \int dr r^2 \sum_{K, P} (2K + 1) \left[g_{11}^{(2)} + g_{22}^{(2)} + g_{33}^{(2)} + g_{44}^{(2)} \right] , \quad (3.22)$$

where the Green functions are taken at $r = r'$. Analogously, the functional derivative of the energy is obtained as

$$\begin{aligned} \left. \frac{\delta E_0^{(2)}}{\delta \phi_a(\mathbf{z})} \right|_{\phi(\mathbf{z})=\hat{\mathbf{z}}\vartheta(r)} &= m_0 \frac{N_c}{4\pi^2} \hat{z}_a \sum_{K, P} (-1)^K P \\ &\times \int_0^\infty d\nu \left\{ \sin(\vartheta(r)) \left[(2K + 1) \left(-g_{12}^{(1)} + g_{34}^{(1)} + \frac{2}{r} \left\{ -g_{12}^{(1)} + g_{34}^{(1)} \right\} \right) \right] \right. \\ &- \cos(\vartheta(r)) \left[\frac{1}{2} \left(-g_{11}^{(1)} + g_{22}^{(1)} - g_{33}^{(1)} + g_{44}^{(1)} \right) \right. \\ &+ \frac{1}{r} \left((K - 1)g_{11}^{(1)} + (K + 1)g_{22}^{(1)} + Kg_{33}^{(1)} + (K + 2)g_{44}^{(1)} \right) \\ &\left. \left. + 2\sqrt{K(K + 1)} \left(-g_{14}^{(1)} - g_{23}^{(1)} - \frac{1}{r} \left\{ 3g_{14}^{(1)} + g_{23}^{(1)} \right\} \right) \right] \right\} . \end{aligned} \quad (3.23)$$

Both expressions have to be regulated as implied by Eq. (3.15).

The NJL-soliton is a system with baryon number equal to one. Therefore, one has to add the bound state part of the fermionic energy

$$E_0^{\text{comp}} = N_c E^{\text{bou}} + E_0^{(2)} . \quad (3.24)$$

The eigenvalue equation for the bound state reads

$$[-\Delta + \mathcal{V}^{0^+}(\mathbf{x})] \psi_0 = \omega_0^2 \psi_0 . \quad (3.25)$$

³We omit the K-spin and parity superscripts here.

For $K^P = 0^+$ the spinor ψ_0 is determined by two radial wave functions $h(r)$ and $j(r)$, and the potential \mathcal{V}^{0+} is a 2×2 matrix given in Appendix A. The eigenfunctions are normalized as $\int |\psi_0(\mathbf{x})|^2 d^3x = 1$. Differentiating the bound state equation with respect to $\phi_a(\mathbf{z})$ and projecting with ψ_0^\dagger one finds

$$\frac{\delta}{\delta \phi_a(\mathbf{z})} \omega_0 = \frac{1}{2\omega_0} \int d^3x \psi_0^\dagger(\mathbf{x}) \frac{\delta \mathcal{V}^{0+}(\mathbf{x})}{\delta \phi_a(\mathbf{z})} \psi_0(\mathbf{x}). \quad (3.26)$$

Inserting the explicit expressions for the potential and the eigenfunctions, the derivative of the bound state energy takes the form

$$\frac{\delta E^{\text{bou}}}{\delta \phi_a(\mathbf{z})} \Big|_{\phi(\mathbf{z})=\hat{\mathbf{z}}^{\vartheta(r)}} = m_0 \frac{N_c}{4\pi\omega_0} \hat{z}_a \left\{ \sin(\vartheta(r)) \left[h'(r)j(r) + j'(r)h(r) + \frac{2}{r}h(r)j(r) \right] \right. \\ \left. - \cos(\vartheta(r)) \left[-h'(r)h(r) + j'(r)j(r) + \frac{2}{r}j^2(r) \right] \right\}. \quad (3.27)$$

The bound state energy is convergent. Thus it does not need to be regularized. With a finite regulator, however, this is subject to some arbitrariness. The same argument would hold for any finite subset of sea quark states, or of all the finite parts higher order terms of the perturbative expansion.

Finally, the mesonic part of the energy and its derivative have to be evaluated. This is straightforward, as they are given by simple analytical expressions. On the chiral circle one finds

$$E^{\text{br}} = -4\pi m_\pi^2 f_\pi^2 \int dr r^2 [\cos(\vartheta(r)) - 1] \quad (3.28)$$

and

$$\frac{\delta E^{\text{br}}}{\delta \phi_a(\mathbf{z})} \Big|_{\phi(\mathbf{z})=\hat{\mathbf{z}}^{\vartheta(r)}} = m_\pi^2 f_\pi^2 \hat{z}_a \sin(\vartheta(r)). \quad (3.29)$$

4 Perturbative expansion of the Green function

After reduction of Eq. (3.9) to K-spin partial waves (see Appendix A) the differential equation for the partial wave Green functions $g_{mn}(r, r', \nu)$ becomes

$$\left[\delta_{nk} \left(\frac{d^2}{dr^2} + \frac{2}{r} \frac{d}{dr} - \frac{K_n(K_n + 1)}{r^2} - \kappa^2 \right) - \mathcal{V}_{nk}(r) \right] g_{km}(r, r', \nu) \\ = -\delta_{nm} \delta(r - r')/r^2, \quad (4.1)$$

where $\kappa = \sqrt{\nu^2 + m_0^2}$ and where, again, we suppress the partial wave indices K and P . The potential \mathcal{V}_{mn} depends on the K-spin, its explicit form is given in Appendix A. As already mentioned, we use for the numerical computation of the Green functions their standard expression (3.21) in terms of mode functions $f_n^{\alpha\pm}(r)$. The functions $f_n^{\alpha\pm}$ form

4×2 linearly independent systems (index $\alpha\pm$) of 4-component solutions (subscript n). A form independent of the choice of basis is given in [11, 20]. Here we use a special convenient basis; it is defined by splitting off the free solutions, i.e. the modified Bessel functions $b_{K_n}^+(\kappa r) \equiv k_{K_n}(\kappa r)$ and $b_{K_n}^-(\kappa r) \equiv i_{K_n}(\kappa r)$ via

$$f_n^{\alpha\pm}(r) = [\delta_n^{\alpha\pm} + h_n^{\alpha\pm}(r)] b_{K_n}^{\pm}(\kappa r) \quad (4.2)$$

and by imposing the boundary condition

$$\lim_{r \rightarrow \infty} h_n^{\alpha\pm}(r) = 0. \quad (4.3)$$

The truncated mode-functions are obtained by solving the equations

$$\left[\frac{d^2}{dr^2} + 2 \left(\frac{1}{r} + \kappa \frac{b_{K_n}^{\pm}(\kappa r)}{b_{K_n}^{\pm}(\kappa r)} \right) \frac{d}{dr} \right] h_n^{\alpha\pm}(r) = \mathcal{V}_{nm}^K(r) [\delta_m^{\alpha} + h_m^{\alpha\pm}(r)] \frac{b_{K_m}^{\pm}(\kappa r)}{b_{K_n}^{\pm}(\kappa r)}, \quad (4.4)$$

or, in a short form,

$$Dh = \mathcal{V}(1 + h). \quad (4.5)$$

This equation can be used for a perturbative expansion. Obviously, the functions $h_n^{\alpha\pm}(r)$ vanish to zeroth order in \mathcal{V} , so, in the notation introduced in the previous section, they are of order $\overline{(1)}$. Once these solutions are known, the differential equation may be iterated to obtain the contribution of order $\overline{(2)}$ via

$$Dh^{\overline{(1)}} = \mathcal{V}(1 + h^{\overline{(1)}}), \quad (4.6)$$

$$Dh^{\overline{(2)}} = \mathcal{V}h^{\overline{(1)}}. \quad (4.7)$$

In terms of these functions the expression (3.21) becomes, for $r > r'$,

$$g_{nm}^{\overline{(1)}}(r, r') = \frac{\kappa}{2} [h_n^{\overline{(1)m-}}(r') + h_m^{\overline{(1)n+}}(r) + h_n^{\overline{(1)\alpha-}}(r')h_m^{\overline{(1)\alpha+}}(r)] k_{K_m}(r) i_{K_n}(r'), \quad (4.8)$$

$$g_{nm}^{\overline{(2)}}(r, r') = \frac{\kappa}{2} [h_n^{\overline{(2)m-}}(r') + h_m^{\overline{(2)n+}}(r) + h_n^{\overline{(2)\alpha-}}(r')h_m^{\overline{(2)\alpha+}}(r)] k_{K_m}(r) i_{K_n}(r'). \quad (4.9)$$

These expressions are ready for being inserted into Eqs. (3.22) and (3.23). In renormalized perturbation theory one would, using further iterations, reduce these expressions to order $\overline{(3)}$ and evaluate the second order analytically as in Eq. (3.14).

5 Quantization of collective coordinates

The hedgehog system is invariant under K-spin, i.e., under combined space and isospin rotations. For a rotating hedgehog state the Hamiltonian is modified as [31]

$$H_{\Omega}(\boldsymbol{\Omega}) = H(\mathbf{x}) - \frac{1}{2}\boldsymbol{\Omega} \cdot \boldsymbol{\tau} = -i\boldsymbol{\alpha} \cdot \boldsymbol{\nabla} + \gamma_0 \mathbf{m}(\mathbf{x}) - \frac{1}{2}\boldsymbol{\Omega} \cdot \boldsymbol{\tau}, \quad (5.1)$$

where Ω is the angular velocity. Assuming Ω to be small, the problem can be treated perturbatively. The first order in Ω vanishes, in second order one obtains

$$S_{\text{eff}} = -\tau \left[E_0(\Omega) + \frac{1}{2} \Omega_a \theta_{ab} \Omega_b \right], \quad (5.2)$$

where θ_{ab} is the moment of inertia

$$\theta_{ab} = \left. \frac{\delta^2 E_0(\Omega)}{\delta \Omega_a \delta \Omega_b} \right|_{\Omega=0}. \quad (5.3)$$

θ_{ab} is proportional to the unit matrix, $\theta_{ab} = \theta \delta_{ab}$. The collective coordinate can be quantized in the usual way, leading to an extra term $J(J+1)/2\theta$ in the energy.

Taking the second derivative with respect to Ω of the fermion Green function

$$S_E^\Omega(\mathbf{x}, \mathbf{x}', \nu) = -\langle x | \frac{1}{i\nu - H_\Omega(\Omega)} | x' \rangle \quad (5.4)$$

one obtains

$$\begin{aligned} \frac{\delta^2 S_E^\Omega(\mathbf{x}, \mathbf{x}', \nu)}{\delta \Omega_a \delta \Omega_b} &= -\langle x | \frac{1}{i\nu - H_\Omega(\Omega)} \frac{\tau_a}{2} \frac{1}{i\nu - H_\Omega(\Omega)} \frac{\tau_b}{2} \frac{1}{i\nu - H_\Omega(\Omega)} | x' \rangle \\ &\quad - \langle x | \frac{1}{i\nu - H_\Omega(\Omega)} \frac{\tau_b}{2} \frac{1}{i\nu - H_\Omega(\Omega)} \frac{\tau_a}{2} \frac{1}{i\nu - H_\Omega(\Omega)} | x' \rangle \end{aligned} \quad (5.5)$$

$$= -\frac{i}{4} \frac{\partial}{\partial \nu} \langle x | \tau_a \frac{1}{i\nu - H_\Omega(\Omega)} \tau_b \frac{1}{i\nu - H_\Omega(\Omega)} | x' \rangle. \quad (5.6)$$

Inserting this equation in Eq. (3.11) the tensor can be calculated via

$$\left. \frac{\delta^2 E_0}{\delta \Omega_a \delta \Omega_b} \right|_{\Omega=0} = N_c \int_{-\infty}^{\infty} \frac{d\nu}{8\pi} \int d^3x \int d^3x' \text{tr} \left[\tau_a S_E^0(\mathbf{x}, \mathbf{x}', \nu) \tau_b S_E^0(\mathbf{x}', \mathbf{x}, \nu) \right], \quad (5.7)$$

where $S_E^0(\mathbf{x}, \mathbf{x}', \nu)$ is defined by Eq. (3.4). This expression can be rewritten with the "bosonic" Green function (3.9)

$$\begin{aligned} \theta_{ab} &= N_c \int_{-\infty}^{\infty} \frac{d\nu}{8\pi} \int d^3x \int d^3x' \\ &\quad \times \text{tr} \left[\tau_a \{i\nu + H(\mathbf{x})\} G_E(\mathbf{x}, \mathbf{x}', \nu) \tau_b \{i\nu + H(\mathbf{x}')\} G_E(\mathbf{x}', \mathbf{x}, \nu) \right]. \end{aligned} \quad (5.8)$$

The bound state is occupied and, therefore, included into the negative continuum by choosing the dashed integration contour displayed in Fig. 1. If the Green function is expanded into eigenfunctions of the Hamiltonian as in Eq. (3.3), it can be readily verified that this way one obtains transitions between the positive and negative continuum states as well as transitions between the bound state and the positive continuum as discussed in [32]. Here this detailed structure is not explicit.

As for the energy, we will consider the bound state contribution separately. We decompose the dashed contour into a contour running along the real ν axis and a small circle around the bound state pole. We will denote the former contribution which describes the continuum-continuum-transitions by a superscript $c - c$, and the bound state contributions by the superscript $b - c$ as it involves matrix elements between the bound state and the continuum. We begin with considering the continuum contributions.

The partial wave reduction of the Green function $G_E(\mathbf{x}, \mathbf{x}', \nu)$ has been introduced above and is discussed in Appendix A. Here we need the partial wave reduction for the fermion propagator $(i\nu + H)G_E$; we denote the associated matrix elements by $g_{\tilde{m}n}^K(r, r', \nu)$, the index with tilde indicates the application of $(i\nu + H)$ from the left side. This Green function can again be decomposed into mode functions as in Eq. 3.21, one just has to replace the functions $f_n(r)$ by new functions $f_{\tilde{n}}(r)$. These functions are given explicitly in Appendix A. Furthermore, we have to take the trace with isospin matrices τ_a . As $\theta_{ab} \propto \delta_{ab}$ it is sufficient to compute θ_{33} . The action of τ_3 on the K-spin harmonics is given in Appendix B. Using these expressions, the angular integration over $d\Omega_r$ and $d\Omega_{r'}$ and the summation over the third component of K and K' can be performed. K' is fixed by the angular integration to the values K , $K - 1$ or $K + 1$. Finally, one obtains

$$\begin{aligned}
& \int d\Omega_r \int d\Omega_{r'} \text{tr} \left[\tau_3 \{ i\nu + H(\mathbf{x}) \} G_E(\mathbf{x}, \mathbf{x}', \nu) \tau_3 \{ i\nu + H(\mathbf{x}') \} G_E(\mathbf{x}', \mathbf{x}, \nu) \right] = \\
& \sum_{P,K=1}^{\infty} \left[\frac{(K+1)(2K+1)}{3K} \left\{ g_{\tilde{1}1}^K(r, r') g_{\tilde{1}1}^K(r', r) + g_{\tilde{2}2}^K(r, r') g_{\tilde{2}2}^K(r', r) \right. \right. \\
& \quad \left. \left. + g_{\tilde{1}2}^K(r, r') g_{\tilde{2}1}^K(r', r) + g_{\tilde{2}1}^K(r, r') g_{\tilde{1}2}^K(r', r) \right\} \right. \\
& \quad \left. + \frac{(2K+1)K}{3(K+1)} \left\{ g_{\tilde{3}3}^K(r, r') g_{\tilde{3}3}^K(r', r) + g_{\tilde{4}4}^K(r, r') g_{\tilde{4}4}^K(r', r) \right. \right. \\
& \quad \left. \left. + g_{\tilde{3}4}^K(r, r') g_{\tilde{4}3}^K(r', r) + g_{\tilde{4}3}^K(r, r') g_{\tilde{3}4}^K(r', r) \right\} \right. \\
& \quad \left. - \frac{(2K+1)}{3} \left\{ g_{\tilde{1}4}^K(r, r') g_{\tilde{4}1}^K(r', r) + g_{\tilde{4}1}^K(r, r') g_{\tilde{1}4}^K(r', r) \right. \right. \\
& \quad \left. \left. + g_{\tilde{1}3}^K(r, r') g_{\tilde{3}1}^K(r', r) + g_{\tilde{3}1}^K(r, r') g_{\tilde{1}3}^K(r', r) \right. \right. \\
& \quad \left. \left. + g_{\tilde{3}2}^K(r, r') g_{\tilde{2}3}^K(r', r) + g_{\tilde{2}3}^K(r, r') g_{\tilde{3}2}^K(r', r) \right. \right. \\
& \quad \left. \left. + g_{\tilde{2}4}^K(r, r') g_{\tilde{4}2}^K(r', r) + g_{\tilde{4}2}^K(r, r') g_{\tilde{2}4}^K(r', r) \right\} \right. \\
& \quad \left. + \frac{4K^2 - 1}{3K} \left\{ g_{\tilde{2}2}^K(r, r') g_{\tilde{4}4}^{K-1}(r', r) + g_{\tilde{1}2}^K(r, r') g_{\tilde{4}3}^{K-1}(r', r) \right. \right. \\
& \quad \left. \left. + g_{\tilde{2}1}^K(r, r') g_{\tilde{3}4}^{K-1}(r', r) + g_{\tilde{1}1}^K(r, r') g_{\tilde{3}3}^{K-1}(r', r) \right. \right. \\
& \quad \left. \left. + g_{\tilde{3}3}^{K-1}(r, r') g_{\tilde{1}1}^K(r', r) + g_{\tilde{4}4}^{K-1}(r, r') g_{\tilde{2}2}^K(r', r) \right. \right. \\
& \quad \left. \left. + g_{\tilde{3}4}^{K-1}(r, r') g_{\tilde{2}1}^K(r', r) + g_{\tilde{4}3}^{K-1}(r, r') g_{\tilde{1}2}^K(r', r) \right\} \right].
\end{aligned}$$

As we need this expression in order $\overline{(2)}$, the modified Green functions have to be inserted

in order $\overline{(1)}$. One can take advantage of the factorization of the Green functions into mode functions, see A.18, to rewrite this expression in the form

$$\begin{aligned} \theta^{c-c} &= \frac{\delta^2 E_0}{\delta \Omega_a \delta \Omega_b} \Big|_{\Omega=0} = N_c \int_{-\infty}^{\infty} \frac{d\nu}{4\pi} \sum_{P,K=1}^{\infty} \\ &\times \int_0^{\infty} dr r^2 \left[H_{1K}^{+\alpha\beta}(r) \int_0^r dr' r'^2 \left\{ \frac{(K+1)(2K+1)}{3K} H_{1K}^{-\beta\alpha}(r') - \frac{2K+1}{3} H_{2K}^{-\beta\alpha}(r') \right\} \right. \\ &+ H_{2K}^{+\alpha\beta}(r) \int_0^r dr' r'^2 \left\{ \frac{K(2K+1)}{3(K+1)} H_{2K}^{-\beta\alpha}(r') - \frac{2K+1}{3} H_{1K}^{-\beta\alpha}(r') \right\} \\ &+ H_{3K}^{+\alpha\beta}(r) \int_0^r dr' r'^2 \left\{ \frac{4K^2-1}{3K} H_{4K}^{-\beta\alpha}(r') \right\} \\ &\left. + H_{4K}^{+\alpha\beta}(r) \int_0^r dr' r'^2 \left\{ \frac{4K^2-1}{3K} H_{3K}^{-\beta\alpha}(r') \right\} \right]. \end{aligned} \quad (5.9)$$

The functions $H_{iK}^{\pm\alpha\beta}(r)$ are defined as

$$H_{1K}^{\pm\alpha\beta}(r) = \kappa \left[f_{\tilde{1},K}^{\alpha\pm}(r) f_{1,K}^{\beta\pm}(r) + f_{\tilde{2},K}^{\alpha\pm}(r) f_{2,K}^{\beta\pm}(r) \right], \quad (5.10)$$

$$H_{2K}^{\pm\alpha\beta}(r) = \kappa \left[f_{\tilde{3},K}^{\alpha\pm}(r) f_{3,K}^{\beta\pm}(r) + f_{\tilde{4},K}^{\alpha\pm}(r) f_{4,K}^{\beta\pm}(r) \right], \quad (5.11)$$

$$H_{3K}^{\pm\alpha\beta}(r) = \kappa \left[f_{\tilde{1},K}^{\alpha\pm}(r) f_{3,K-1}^{\beta\pm}(r) + f_{\tilde{2},K}^{\alpha\pm}(r) f_{4,K-1}^{\beta\pm}(r) \right], \quad (5.12)$$

$$H_{4K}^{\pm\alpha\beta}(r) = \kappa \left[f_{\tilde{3},K-1}^{\alpha\pm}(r) f_{1,K}^{\beta\pm}(r) + f_{\tilde{4},K-1}^{\alpha\pm}(r) f_{2,K}^{\beta\pm}(r) \right], \quad (5.13)$$

in terms of the mode functions $f_n^{\alpha\pm}$ and $f_{\tilde{n}}^{\alpha\pm}$ defined in (A.1) and (A.14), respectively. One has to combine the orders of $H_i^{\pm\alpha\beta}$ in such a way that the result is of total order $\overline{(2)}$:

$$\theta_{ab}^{c-c\overline{(1)}} \sim H^{+\overline{(1)}} H^{-\overline{(1)}} + H^{+(0)} H^{-\overline{(1)}} + H^{+\overline{(1)}} H^{-(0)}. \quad (5.14)$$

In fact the first order part which has been included on the right hand side for practical convenience vanishes. The functions $H^{\pm\overline{(1)}}$ are obtained as

$$H^{\pm\overline{(1)}} \sim f^{\pm\overline{(1)}} f^{\pm\overline{(1)}} + f^{\pm(0)} f^{\pm\overline{(1)}} + f^{\pm\overline{(1)}} f^{\pm(0)}; \quad (5.15)$$

the functions $H^{\pm(0)}$ are composed of free Bessel functions.

Since the imaginary part of the integral of Eq. (5.9) is antisymmetric, the result equals twice the real part, integrated from $\nu = 0$ up to ∞ . It is implied that the expressions have to be regularized by Pauli-Villars subtractions.

Having presented the continuum-continuum contributions to the moment of inertia we now turn to the bound state contribution. This contribution is given, in terms of eigenfunctions of the Dirac operator by [32, 33]

$$\frac{\partial^2 \omega_0}{\partial \Omega_a \partial \Omega_a} \Big|_{\Omega=0} = \frac{N_c}{2} \sum_{m \neq \text{bou}} \frac{\langle \psi_0 | \tau_a | \psi_m \rangle \langle \psi_m | \tau_b | \psi_0 \rangle}{E^m - E^{\text{bou}}}. \quad (5.16)$$

Using the (3.3) for the Green function we find that this expression for the moment of inertia is identical to

$$\theta_{ab}^{b-c} = \frac{\partial^2 \omega_0}{\partial \Omega_a \partial \Omega_b} \Big|_{\Omega=0} = \frac{N_c}{2} \text{tr} \int d^3x d^3x' \psi_0(\mathbf{x}) \psi_0^\dagger(\mathbf{x}') \tau_a S(\mathbf{x}', \mathbf{x}, -iE^{\text{bou}}) \tau_b. \quad (5.17)$$

The Euclidean Green function at any imaginary argument can again be related to the bosonic Green function via

$$S_E(\mathbf{x}, \mathbf{x}', -iE^{\text{bou}}) = (H + E^{\text{bou}}) G_E(\mathbf{x}, \mathbf{x}', iE^{\text{bou}}). \quad (5.18)$$

Since the energy of the bound state is smaller than the mass m_0 , the calculation of the Green function is analogous to the one for the continuum part, Eq. (5.9), with

$$\kappa^2 = m_0^2 - E_{\text{bou}}^2. \quad (5.19)$$

Furthermore, the valence state 0^+ only couples to $K^P = 1^+$ continuum states. Therefore, the expression for this contribution reduces to

$$\theta_{ab}^{b-c} = \frac{N_c}{2\kappa} \int_0^\infty dr r^2 \left[\mathcal{H}_3^{+\alpha}(r) \int_0^r dr' r'^2 \mathcal{H}_4^{-\alpha}(r') + \mathcal{H}_4^{+\alpha}(r) \int_0^r dr' r'^2 \mathcal{H}_3^{-\alpha}(r') \right] \quad (5.20)$$

with

$$\mathcal{H}_3^{\pm\alpha}(r) = \kappa \left[f_{\tilde{1},1}^{\alpha\pm}(r) h(r) + f_{\tilde{2},1}^{\alpha\pm}(r) j(r) \right], \quad (5.21)$$

$$\mathcal{H}_4^{\pm\alpha}(r) = \kappa \left[f_{1,1}^{\alpha\pm}(r) h(r) + f_{2,1}^{\alpha\pm}(r) j(r) \right]. \quad (5.22)$$

As for the bound state contribution to the energy, this part of the moment of inertia is finite and will not be Pauli-Villars subtracted. Adding the $c - c$ and $b - c$ contributions the moment of inertia is given by

$$\theta = \theta^{b-c} + \theta^{c-c}(m_0) - \frac{m_0^2}{\Lambda^2} \theta^{c-c}(\Lambda). \quad (5.23)$$

Proceeding in an analogous way one can obtain expressions for the expectation values of other observables as well. Expressions for $\langle \Sigma_3 \rangle$ and $\langle L_3 \rangle$ in terms of mode sums have been derived in [33]. The spin expectation value is given by

$$\langle \Sigma_3 \rangle = -\frac{1}{\theta} \frac{N_c}{2} \sum_{m,n} \frac{\langle \psi_n | \tau_3 | \psi_m \rangle \langle \psi_m | \Sigma_3 | \psi_n \rangle}{E_m - E_n}. \quad (5.24)$$

It can be rewritten in terms of the Euclidean Green function as

$$\langle \Sigma_3 \rangle = -\frac{N_c}{\theta} \int_{-\infty}^{\infty} \frac{d\nu}{8\pi} \int d^3x \int d^3x' \text{tr} \left[\tau_3 S_E^0(\mathbf{x}, \mathbf{x}', \nu) \sigma_3 S_E^0(\mathbf{x}', \mathbf{x}, \nu) \right] \quad (5.25)$$

where the contour again includes the bound state. The bound state and continuum contributions are obtained separately, as above.

6 Observables

The expressions for the energy and for the moment of inertia have already been presented. The mass of the low-lying baryons with K-spin 0 is given by the sum of static and rotational energy as

$$M_J = E_0 + \frac{J(J+1)}{2\theta}, \quad (6.1)$$

therefore

$$M_N = E_0 + \frac{3}{8\theta} \quad (6.2)$$

and

$$M_\Delta - M_N = \frac{15}{8\theta} - \frac{3}{8\theta} = \frac{3}{2\theta}. \quad (6.3)$$

The nucleon sigma term is defined as

$$\Sigma = m_0 \int d^3x \langle \bar{q}q \rangle. \quad (6.4)$$

As shown in [34] it is given simply by the symmetry breaking part of the energy as

$$\Sigma = E^{\text{br}}. \quad (6.5)$$

The experimental value is 45 ± 9 MeV [35]. The pion-nucleon coupling constant can be obtained [6] from the long range behavior of the meson profile

$$C = f_\pi \lim_{r \rightarrow \infty} r^2 \sin(\vartheta) \frac{\exp(m_\pi r)}{1 + m_\pi r} \quad (6.6)$$

as

$$g_{\pi NN} = \frac{8}{3} \pi M_N C. \quad (6.7)$$

The axial vector coupling constant is given [33, 37] by the expectation value

$$g_A = \langle p \uparrow | \gamma_0 \tau_3 \gamma_3 \gamma_5 | p \uparrow \rangle. \quad (6.8)$$

It consists of a valence state contribution

$$\begin{aligned} g_A^{\text{bou}} &= -\frac{N_c}{3} \text{tr} \int d^3x (\gamma_0 \gamma_3 \gamma_5 \tau_3) \psi_0(\mathbf{x}) \psi_0^\dagger(\mathbf{x}) \\ &= \frac{N_c}{3} \int dr r^2 \left[h^2(r) - \frac{1}{3} j^2(r) \right] \end{aligned} \quad (6.9)$$

and a continuum part which, using the Euclidean Green function, can be written as

$$\begin{aligned} g_A^{\text{con}} &= -\frac{N_c}{3} \text{tr} \int d^3x \int_{-\infty}^{\infty} \frac{d\nu}{2\pi} (\gamma_0 \gamma_3 \gamma_5 \tau_3) S_E(\mathbf{x}, \mathbf{x}, \kappa) \\ &= -\frac{2}{9} N_c \int_0^\infty \frac{d\nu}{2\pi} \int_0^\infty dr r^2 \sum_{K^P} \left[(2K+1) g_{\tilde{1},1}(r, r, \kappa) - (2K-1) g_{\tilde{2},2}(r, r, \kappa) \right. \\ &\quad \left. - (2K+3) g_{\tilde{3},3}(r, r, \kappa) + (2K+1) g_{\tilde{4},4}(r, r, \kappa) \right. \\ &\quad \left. + 4\sqrt{K(K+1)} \{ g_{\tilde{2},3}(r, r, \kappa) + g_{\tilde{3},2}(r, r, \kappa) \} \right]. \end{aligned} \quad (6.10)$$

Pauli-Villars subtraction is implied. With the Goldberger-Treiman relation the axial vector coupling constant can also be calculated via

$$g_A^{G-T} = \frac{f_\pi}{M_N} g_{\pi NN} . \quad (6.11)$$

The quadratic radius of

$$\langle R^2 \rangle_{\text{bou}} = \int_0^\infty r^4 dr \{ h^2(r) + j^2(r) \} , \quad (6.12)$$

$$\langle R^2 \rangle_{\text{con}} = \frac{-1}{2\pi} \int_0^\infty d\nu \int_0^\infty r^4 dr \sum_{K^P} \{ g_{\tilde{1}1} + g_{\tilde{2}2} + g_{\tilde{3}3} + g_{44} \} \quad (6.13)$$

has to be compared with an experimental value of 0.62 fm^2 . The continuum part is convergent, but so small that regularizing the integral does not change the result.

7 Numerics

We have numerically implemented the expressions for the energy and its functional derivative presented in section 3 in the way described in [11] for the energy, and in [20] for its functional derivative.

The iteration proceeds as follows: For a given meson profile $\vartheta(r)$ one computes the mode functions and evaluates the functional derivative of the energy. One then requires the vanishing of the functional derivative,

$$\hat{z}_a \left(\frac{\delta E_{0,m}^{(2)}}{\delta \phi_a(\mathbf{z})} + \frac{\delta E^{\text{bou}}}{\delta \phi_a(\mathbf{z})} + \frac{\delta E^{\text{br}}}{\delta \phi_a(\mathbf{z})} - \frac{m^2}{\Lambda^2} \frac{\delta E_{0,\Lambda}^{(2)}}{\delta \phi_a(\mathbf{z})} \right)_{\phi(\mathbf{z})=\hat{\mathbf{z}}\vartheta(r)} = 0 . \quad (7.1)$$

As can be seen from Eqs. (3.23), (3.27) and (3.29), this equation takes the form

$$\left. \frac{\delta E}{\delta \phi_a(\mathbf{z})} \right|_{\phi(\mathbf{z})=\hat{\mathbf{z}}\vartheta(r)} = \hat{z}_a [A(r) \cos(\vartheta(r)) + B(r) \sin(\vartheta(r))] . \quad (7.2)$$

The coefficient functions $A(r)$ and $B(r)$ are the results of the numerical computation. Extremizing the energy by requiring the functional derivative to vanish fixes $\vartheta(r)$ via $\tan(\vartheta(r)) = -A(r)/B(r)$. This profile is used as the input for the next iteration. This method of iteration has been used previously by [37].

The functions $h^{\alpha\pm}(r)$ have been computed in order $(\overline{1})$ and $(\overline{2})$ by solving (4.4) and its recursion (4.7) using a Runge-Kutta scheme. The accuracy of these solutions was checked by using the Wronskian relation, which was constant to at least 6 significant units. The sum over the K-spin was extended to $K = 16$ during the iteration and to $K = 20$ for the final result. The sum over the higher angular momenta was appended using a power fit to the terms computed numerically. The range of the Euclidean energy was $\nu < 5$, again the integration over higher values was appended using a power fit.

The numerical results for the energy and other static parameters are presented in Table 1. and in Figs. 2-6.

8 Results and conclusions

We have presented here a self-consistent computation of the nucleon ground state in the Nambu-Jona-Lasinio model. In contrast to most previous calculations we have used a Pauli-Villars cutoff. It has been shown recently [8] that such a cutoff is favored by parton sum rules. As the main object of this work we have introduced an alternative method of numerical computation, based on Euclidean Green functions instead of the use of the quark eigenfunctions for real energies. Our method has the advantage that it is not necessary to discretize the continuous spectrum of the sea quarks. While this discretization and the associated limiting procedure seem to be well under control, finite boundaries may introduce spurious effects, as discussed in [33]. Although our results essentially confirm those of other groups, this agreement is by no means guaranteed.

Besides presenting the analytical framework for the computation of self-consistent profiles, based on explicit expressions for the energy and its functional derivative, we have also derived explicit expressions for other observables. Again the quark sea contributions can be formulated in terms of the Euclidean Green function.

Our numerical results are presented in Table 1 and plotted in Figs. 2-6. In Table 1 we also give some results obtained for $g = 4$ in Ref. [7], when using the same regularization. In view of the difference of the numerical approaches the agreement is very satisfactory. This agreement holds as well for the mesonic profiles $\pi(r)$, plotted in Fig. 2. In Figs. 3-6 we plot the various parts of the energy, the axial vector coupling g_A , the mesonic profiles $\vartheta(r)$ and the moment of inertia, as functions of the coupling g . One sees that a value of $g \simeq 4$ is preferred by the comparison with experiment.

The nucleon mass is still too high, but lower than the one obtained with Schwinger proper-time cutoff. A lower value for M_N can be obtained by minimizing the sum of fluctuation energy and rotational energy [38]. We have not followed this issue here. A major improvement is observed for the axial coupling constant g_A which is computed from the quark current, and for which we obtain values between 1.15 and 1.37 as shown in Fig. 5. In contrast, the values obtained with Schwinger proper-time cutoff are well below 1. Similar values for g_A have been obtained recently using a Gaussian cutoff by Golli *et al.* [28]. The bound state contribution agrees with the one given in [7]. The major part of the increase of g_A with g comes from the continuum part. The values for g_A obtained from the asymptotic behavior of the soliton profile via the Goldberger-Treiman relation are somewhat lower than those computed directly from the quark currents, they are in the range between 1.15 and 1.17.

In conclusion we have presented here a new approach to computing self-consistent meson profiles and static observables of the nucleon in the Nambu-Jona-Lasinio model, using a Pauli-Villars cutoff. The agreement with previous analyses using the same cutoff but different numerical methods is very satisfactory, some results given here are new. In view of the fact that our numerical procedure is rather economical we think that it is worthwhile to pursue its application, e.g., to alternative versions of the model or to similar self-consistency problems.

Acknowledgements

H.S. thanks the Graduiertenkolleg "Erzeugung und Zerfälle von Elementarteilchen" for financial support.

A Partial waves and relations of the spinor-isospinors

The expansion with respect to K-spin harmonics Ξ_{ij}

$$\psi_{K,K_z,P}(\mathbf{x}) = \begin{pmatrix} f_1^{K,P}(r) \Xi_1^{K,K_z}(\hat{\mathbf{x}}) + f_4^{K,P}(r) \Xi_4^{K,K_z}(\hat{\mathbf{x}}) \\ f_2^{K,P}(r) \Xi_2^{K,K_z}(\hat{\mathbf{x}}) + f_3^{K,P}(r) \Xi_3^{K,K_z}(\hat{\mathbf{x}}) \end{pmatrix} \quad \text{for parity } (-1)^{(K+1)} \quad (\text{A.1})$$

reduces the Dirac equation to radial equations for four coupled partial waves f_i . The Hamiltonian

$$H_{ij}^{K^P} f_j = E f_i \quad (\text{A.2})$$

for parity $(-1)^{(K+1)}$ is given by

$$\mathcal{H}^{K^P} = \begin{Bmatrix} 0 & -\frac{d}{dr} - \frac{K+1}{r} & 0 & 0 \\ \frac{d}{dr} - \frac{K-1}{r} & 0 & 0 & 0 \\ 0 & 0 & 0 & -\frac{d}{dr} - \frac{K+2}{r} \\ 0 & 0 & \frac{d}{dr} - \frac{K}{r} & 0 \end{Bmatrix} \quad (\text{A.3})$$

$$+ \begin{Bmatrix} C & -cS & sS & 0 \\ -cS & -C & 0 & -sS \\ sS & 0 & -C & -cS \\ 0 & -sS & -cS & C \end{Bmatrix}, \quad (\text{A.4})$$

where

$$S = m_0 \sin(\vartheta(r)), \quad (\text{A.5})$$

$$C = m_0 \cos(\vartheta(r)), \quad (\text{A.6})$$

$$s = 2\sqrt{K(K+1)}/(2K+1), \quad (\text{A.7})$$

$$c = 1/(2K+1). \quad (\text{A.8})$$

This Hamiltonian is squared in order to obtain a bosonic equation. One yields

$$(-\Delta_{ij}^K + m_0^2 \delta_{ij} + \mathcal{V}_{ij}^K) f_j = E^2 f_i, \quad (\text{A.9})$$

where

$$\Delta_{ij}^K = \delta_{ij} \frac{1}{r^2} \frac{d}{dr} r^2 \frac{d}{dr} - \frac{K_i(K_i+1)}{r^2}. \quad (\text{A.10})$$

The notation K_i means $K_1 = K-1$, $K_2 = K_3 = K$ and $K_4 = K+1$. The potential for the parity $(-1)^{K+1}$ is given by

$$\mathcal{V}^K = \begin{Bmatrix} c \left(S' + \frac{2KS}{r} \right) & C' & 0 & s \left(S' - \frac{S}{r} \right) \\ C' & c \left(-S' + \frac{2KS}{r} \right) & s \left(S' + \frac{S}{r} \right) & 0 \\ 0 & s \left(S' + \frac{S}{r} \right) & c \left(S' + \frac{2(K+1)S}{r} \right) & -C' \\ s \left(S' - \frac{S}{r} \right) & 0 & -C' & c \left(-S' + \frac{2(K+1)S}{r} \right) \end{Bmatrix}, \quad (\text{A.11})$$

where

$$S' = m_0 \frac{d}{dr} \sin(\vartheta(r)), \quad (\text{A.12})$$

$$C' = m_0 \frac{d}{dr} \cos(\vartheta(r)). \quad (\text{A.13})$$

For the parity $(-1)^K$ the sign of the mass has to be changed. With the fermionization one obtains the same structure as in Eq. (A.1), but the radial parts change into

$$f_{\tilde{1}} = (i\nu + C) f_1 - \frac{K+1}{r} f_2 - f'_2 - cS f_2 + sS f_3, \quad (\text{A.14})$$

$$f_{\tilde{2}} = (i\nu - C) f_2 - \frac{K-1}{r} f_1 + f'_1 - cS f_1 - sS f_4, \quad (\text{A.15})$$

$$f_{\tilde{3}} = (i\nu - C) f_3 - \frac{K+2}{r} f_4 - f'_4 - cS f_4 + sS f_1, \quad (\text{A.16})$$

$$f_{\tilde{4}} = (i\nu + C) f_4 - \frac{K}{r} f_3 + f'_3 - cS f_3 - sS f_2 \quad (\text{A.17})$$

for the parity $(-1)^{(K+1)}$, thus the Green function becomes complex. With these radial functions the fermionic Green function reads

$$g_{\tilde{n}m}(r, r') = \kappa \left[\theta(r - r') f_{\tilde{n}}^{\alpha+}(r) f_m^{\alpha-}(r') + \theta(r' - r) f_{\tilde{n}}^{\alpha-}(r) f_m^{\alpha+}(r') \right]. \quad (\text{A.18})$$

B K-spin harmonics

The effect of τ_3 , σ_3 and $\sigma_3 \tau_3$ on the K-spin harmonics [30] is

$$\begin{aligned} \tau_3 \Xi_1^{K, K_z} &= \frac{K_z}{K} \Xi_1^{K, K_z} - \frac{\sqrt{K^2 - K_z^2}}{K} \Xi_3^{K-1, K_z}, \\ \tau_3 \Xi_2^{K, K_z} &= \frac{K_z}{K} \Xi_2^{K, K_z} - \frac{\sqrt{K^2 - K_z^2}}{K} \Xi_4^{K-1, K_z}, \\ \tau_3 \Xi_3^{K, K_z} &= -\frac{K_z}{K+1} \Xi_3^{K, K_z} - \frac{\sqrt{(K+1)^2 - K_z^2}}{K+1} \Xi_1^{K+1, K_z}, \\ \tau_3 \Xi_4^{K, K_z} &= -\frac{K_z}{K+1} \Xi_4^{K, K_z} - \frac{\sqrt{(K+1)^2 - K_z^2}}{K+1} \Xi_2^{K+1, K_z}, \end{aligned} \quad (\text{B.1})$$

$$\begin{aligned} \sigma_3 \Xi_1^{K, K_z} &= \frac{K_z}{K} \Xi_1^{K, K_z} - 2 \frac{\sqrt{K-1} \sqrt{K^2 - K_z^2}}{(2K-1)\sqrt{K}} \Xi_2^{K-1, K_z} + \frac{\sqrt{K^2 - K_z^2}}{(2K-1)K} \Xi_3^{K-1, K_z}, \\ \sigma_3 \Xi_2^{K, K_z} &= -2 \frac{\sqrt{K} \sqrt{(K+1)^2 - K_z^2}}{(2K+1)\sqrt{K+1}} \Xi_1^{K+1, K_z} - \frac{K_z(2K-1)}{K(2K+1)} \Xi_2^{K, K_z} \end{aligned}$$

$$\begin{aligned}
& + 2 \frac{K_z}{(2K+1)\sqrt{K(K+1)}} \Xi_3^{K,K_z} - \frac{\sqrt{K^2 - K_z^2}}{K(2K+1)} \Xi_4^{K-1,K_z}, \\
\sigma_3 \Xi_3^{K,K_z} &= \frac{\sqrt{(K+1)^2 - K_z^2}}{(2K+1)(K+1)} \Xi_1^{K+1,K_z} + 2 \frac{K_z}{(2K+1)\sqrt{K(K+1)}} \Xi_2^{K,K_z} \\
& + \frac{K_z(2K+3)}{(2K+1)(K+1)} \Xi_3^{K,K_z} - 2 \frac{\sqrt{K^2 - K_z^2} \sqrt{K+1}}{(2K+1)\sqrt{K}} \Xi_4^{K-1,K_z}, \\
\sigma_3 \Xi_4^{K,K_z} &= - \frac{\sqrt{(K+1)^2 - K_z^2}}{(2K+3)(K+1)} \Xi_2^{K+1,K_z} \\
& - 2 \frac{\sqrt{(K+1)^2 - K_z^2} \sqrt{K+2}}{(2K+3)\sqrt{K+1}} \Xi_3^{K+1,K_z} - \frac{K_z}{K+1} \Xi_4^{K,K_z},
\end{aligned}$$

$$\begin{aligned}
\sigma_3 \tau_3 \Xi_1^{K,K_z} &= - \frac{K - 2K_z^2}{K(2K-1)} \Xi_1^{K,K_z} - 2 \frac{K_z \sqrt{K^2 - K_z^2}}{(2K-1)\sqrt{K(K-1)}} \Xi_2^{K-1,K_z} \\
& - 2 \frac{K_z \sqrt{K^2 - K_z^2}}{K(2K-1)} \Xi_3^{K-1,K_z} + 2 \frac{\sqrt{(K^2 - K_z^2)((K-1)^2 - K_z^2)}}{(2K-1)\sqrt{K(K-1)}} \Xi_4^{K-2,K_z}, \\
\sigma_3 \tau_3 \Xi_2^{K,K_z} &= - 2 \frac{K_z \sqrt{(K+1)^2 - K_z^2}}{(2K+1)\sqrt{K(K+1)}} \Xi_1^{K+1,K_z} + \frac{K - 2K_z^2}{K(2K+1)} \Xi_2^{K,K_z} \\
& + 2 \frac{K^2 + K - K_z^2}{(2K+1)\sqrt{K(K+1)}} \Xi_3^{K,K_z} + 2 \frac{K_z \sqrt{K^2 - K_z^2}}{K(2K+1)} \Xi_4^{K-1,K_z}, \\
\sigma_3 \tau_3 \Xi_3^{K,K_z} &= - 2 \frac{K_z \sqrt{(K+1)^2 - K_z^2}}{(2K+1)(K+1)} \Xi_1^{K+1,K_z} + 2 \frac{K^2 + K - K_z^2}{(2K+1)\sqrt{K(K+1)}} \Xi_2^{K,K_z} \\
& - \frac{K + 1 + 2K_z^2}{(2K+1)(K+1)} \Xi_3^{K,K_z} + 2 \frac{K_z \sqrt{K^2 - K_z^2}}{(2K+1)\sqrt{K(K+1)}} \Xi_4^{K-1,K_z}, \\
\sigma_3 \tau_3 \Xi_4^{K,K_z} &= 2 \frac{\sqrt{((K+1)^2 - K_z^2)((K+2)^2 - K_z^2)}}{(2K+3)\sqrt{(K+1)(K+2)}} \Xi_1^{K+2,K_z} \\
& + 2 \frac{K_z \sqrt{(K+1)^2 - K_z^2}}{(2K+3)(K+1)} \Xi_2^{K+1,K_z} \\
& + 2 \frac{K_z \sqrt{(K+1)^2 - K_z^2}}{(2K+3)\sqrt{(K+1)(K+2)}} \Xi_3^{K+1,K_z} + \frac{1 + K + 2K_z^2}{(2K+3)(K+1)} \Xi_4^{K,K_z}.
\end{aligned}$$

References

- [1] Y. Nambu and G. Jona-Lasinio, Phys. Rev. **122**, 345 (1961)
- [2] *ibid.* **124**, 246 (1961)
- [3] For recent reviews see: R. Alkofer, H. Reinhardt, and H. Weigel, Phys. Rept. **265**, 139 (1996), hep-ph/9501213
- [4] C. Christov *et al.*, Prog. Part. Nucl. Phys. **A5**, 1 (1996), hep-ph/9604441
- [5] T. Skyrme, Proc. Roy. Soc. Lond. **A260**, 127 (1961)
- [6] G. Adkins, C. Nappi, and E. Witten, Nucl. Phys. **B228**, 552 (1983)
- [7] F. Döring *et al.*, Nucl. Phys. **A536**, 548 (1992)
- [8] D. Diakonov, V. Petrov, P. Pobylitsa, M. Polyakov, and C. Weiss, Nucl. Phys. **B480**, 341 (1996), hep-ph/9606314
- [9] J. Baacke, Z. Phys. **C47**, 263 (1990)
- [10] *ibid.* **C47**, 619 (1990)
- [11] J. Baacke, Z. Phys. **C53**, 402 (1992)
- [12] J. Baacke and S. Junker, Phys. Rev. **D49**, 2055 (1994), hep-ph/9308310
- [13] J. Baacke and T. Daiber, Phys. Rev. **D51**, 795 (1995), hep-th/9408010
- [14] L. Carson and L. McLerran, Phys. Rev. **D41**, 647 (1990)
- [15] L. Carson, X. Li, L. McLerran, and R.-T. Wang, Phys. Rev. **D42**, 2127 (1990)
- [16] D. Diakonov *et al.*, Phys. Lett. **B336**, 457 (1994), hep-ph/9407238
- [17] B. Moussallam, Phys. Rev. **D40**, 3430 (1989)
- [18] H. Reinhardt and R. Wünsch, Phys. Lett. **B215**, 577 (1988)
- [19] T. Meissner, F. Grümmer, and K. Goeke, Phys. Lett. **B227**, 296 (1989)
- [20] J. Baacke and A. Surig, Z. Phys. **C73**, 369 (1997), hep-ph/9511231
- [21] A. Sübrig, Phys. Rev. **D57**, 5049 (1998), hep-ph/9706259
- [22] U. Zückert, R. Alkofer, H. Reinhardt, and H. Weigel, Nucl. Phys. **A570**, 445 (1994), hep-ph/9303271
- [23] F. Döring, C. Schüren, E. R. Arriola, and K. Goeke, Phys. Lett. **B298**, 11 (1993)

- [24] M. Lacombe, B. Loiseau, R. V. Mau, and W. N. Cottingham, Phys. Rev. Lett. **57**, 170 (1986)
- [25] M. Chemtob, Nucl. Phys. **A466**, 509 (1987)
- [26] J. Baacke, D. E. L. Pottinger, and M. Golterman, Phys. Lett. **185B**, 421 (1987)
- [27] J. Baacke and H. Lange, Z. Phys. **C39**, 575 (1988)
- [28] B. Golli, W. Broniowski, and G. Ripka, (1998), hep-ph/9807261
- [29] P. Pobylitsa, M. Polyakov, K. Goeke, T. Watabe, and C. Weiss, (1998), hep-ph/9804436
- [30] S. Kahana and G. Ripka, Nucl. Phys. **A429**, 462 (1984)
- [31] D. Diakonov, V. Petrov, and P. Pobylitsa, Nucl. Phys. **B306**, 809 (1988)
- [32] K. Goeke *et al.*, Phys. Lett. **B256**, 321 (1991)
- [33] M. Wakamatsu and H. Yoshiki, Nucl. Phys. **A524**, 561 (1991)
- [34] T. Meissner, F. Grümmer, and K. Goeke, Annals Phys. **202**, 297 (1990)
- [35] J. Gasser, H. Leutwyler, and M. E. Sainio, Phys. Lett. **B253**, 252 (1991)
- [36] M. E. Sainio, Pin Newslett. , NO.1013 (1995)
- [37] T. Meissner and K. Goeke, Nucl. Phys. **A524**, 719 (1991)
- [38] M. Schleif, R. Wünsch, and T. Meissner, (1997), nucl-th/9703024
- [39] E. Matsinos, (1998), hep-ph/9807395.

Table captions

Table 1: Static properties of the nucleons.

Figure captions

Figure 1: The complex ν -plane: Solid line: the contour C_- around the negative continuum states; dashed line: the deformed contour along the real ν axis, including, in addition, the bound state.

Figure 2: The mesonic profile of the nucleon. We display the pion field $\pi = f_\pi \sin(\vartheta)$ as a function of r for $g = 4.0$ (solid line). For comparison we also plot the result obtained previously by Döring *et al.* [7] using a different technique (dots).

Figure 3: The energy of the nucleon. We display the energy as a function of g (solid line), the bound state energy (dotted line), the zero point energy (dashed line) and the energy of the symmetry breaking term (long dashed line). For comparison we also plot the total energy and its parts obtained previously by Döring *et al.* [7] for $g = 4$ (dot, square, diamond and cross).

Figure 4: The axial vector coupling constant. We display the axial vector coupling constant as a function of g . The squares are obtained by calculating the expectation value, the dots by using the Goldberger-Treiman relation. The solid line is the experimental value.

Figure 5: The mesonic profile. We display the mesonic profile ϑ as a function of r for different coupling constants. ($g = 3.8$ solid line, $g = 4.0$ dotted line, $g = 4.2$ dashed line, $g = 4.4$ long dashed line, $g = 4.6$ dash-dotted line)

Figure 6: The moment of inertia. We display the moment of inertia θ as a function for different coupling constants (dots). The solid line is the experimental value.

g		3.8	4.0	4.2	4.4	4.6	4.0 [7]	Exp.
E_{bou}	[MeV]	555	508	464	424	386	507	
E_{con}	[MeV]	549	582	610	634	655	579	
Σ	[MeV]	53	55	57	58	58	52	45 ± 9 [35]
E_{total}	[MeV]	1157	1145	1131	1116	1099	1139	
$1/\theta^{\text{b-c}}$	[MeV]	199	218	233	247	259		
$1/\theta^{\text{c-c}}$	[MeV]	1404	1264	1141	711	575		
$1/\theta_{\text{total}}$	[MeV]	174	186	193	183	178		
$M_{\Delta} - M_N$	[MeV]	261	279	290	274	267		294
M_N	[MeV]	1222	1214	1203	1184	1166		939
$\langle R^2 \rangle_{\text{bou}}$	[fm]	0.56	0.56	0.58	0.60	0.62		
$\langle R^2 \rangle_{\text{con}}$	[fm]	0.001	0.002	0.003	0.004	0.005		
$\langle R^2 \rangle_{\text{total}}$	[fm]	0.56	0.56	0.58	0.60	0.62	0.58	0.62
g_A^{bou}		0.72	0.71	0.71	0.70	0.70	0.71	
g_A^{con}		0.43	0.49	0.55	0.61	0.67		
g_A^{total}		1.15	1.20	1.25	1.31	1.37		1.23
$g_{\pi\text{NN}}$		11.6	11.7	11.8	11.8	11.8		13.1 [39]
$g_A^{\text{G-T}}$		1.15	1.16	1.16	1.16	1.17	0.96	1.23

Table 1

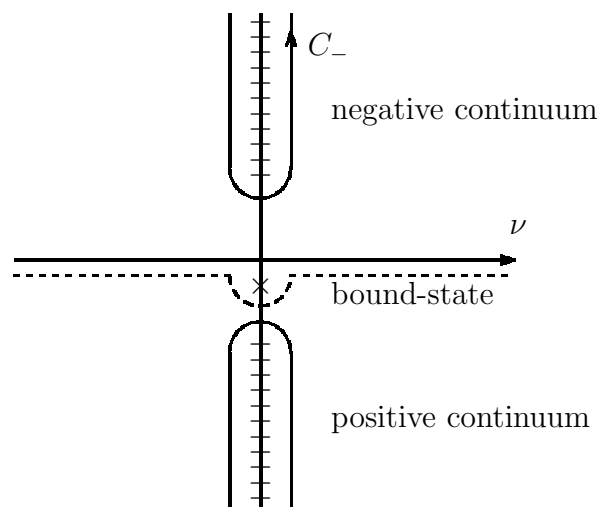


Fig. 1

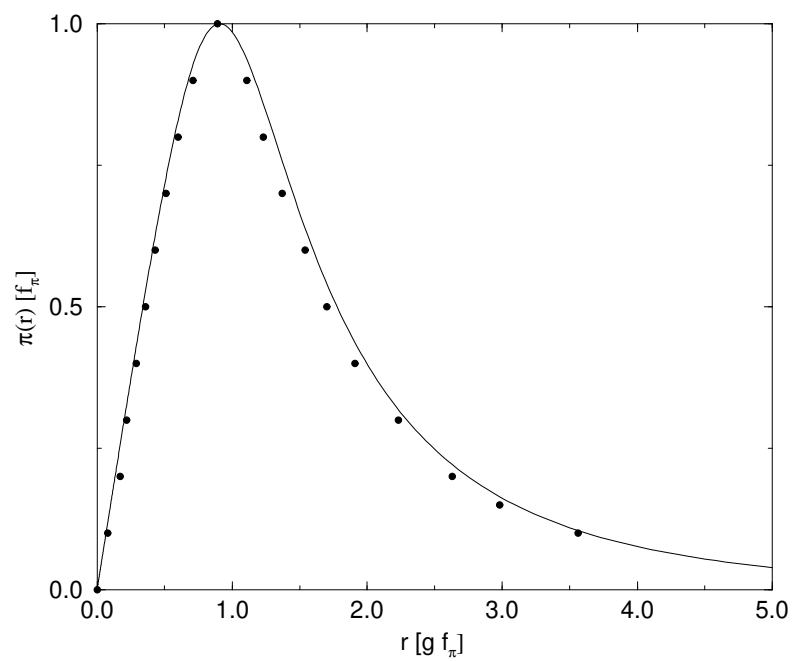


Fig. 2

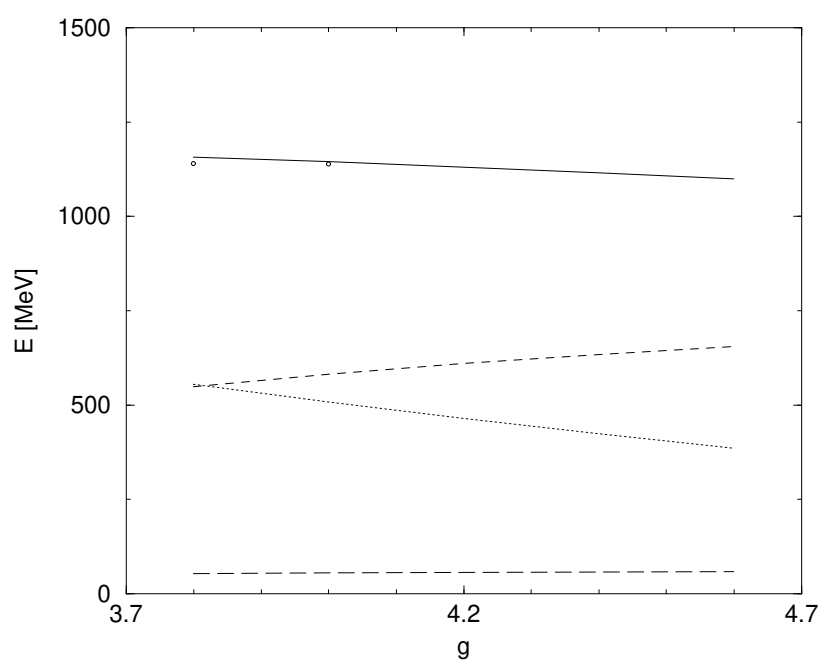


Fig. 3

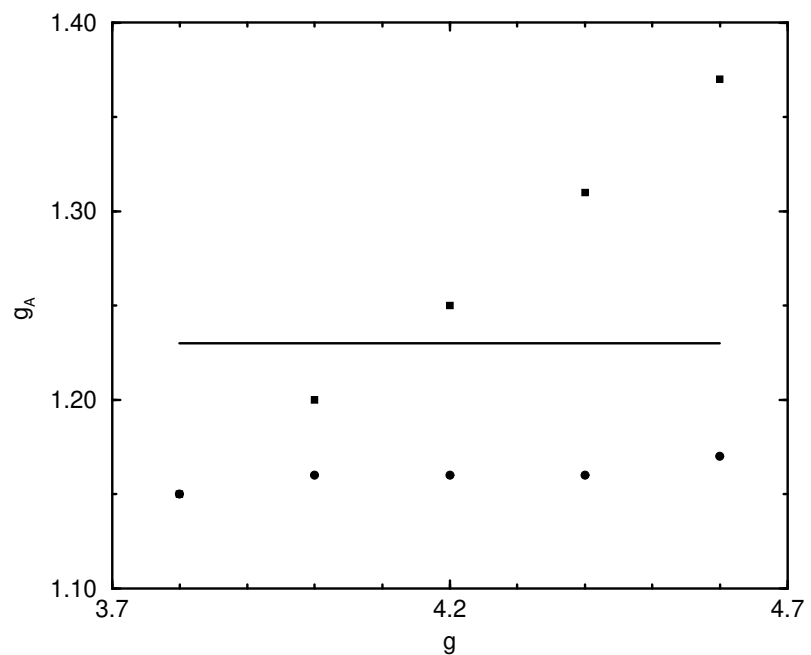


Fig. 4

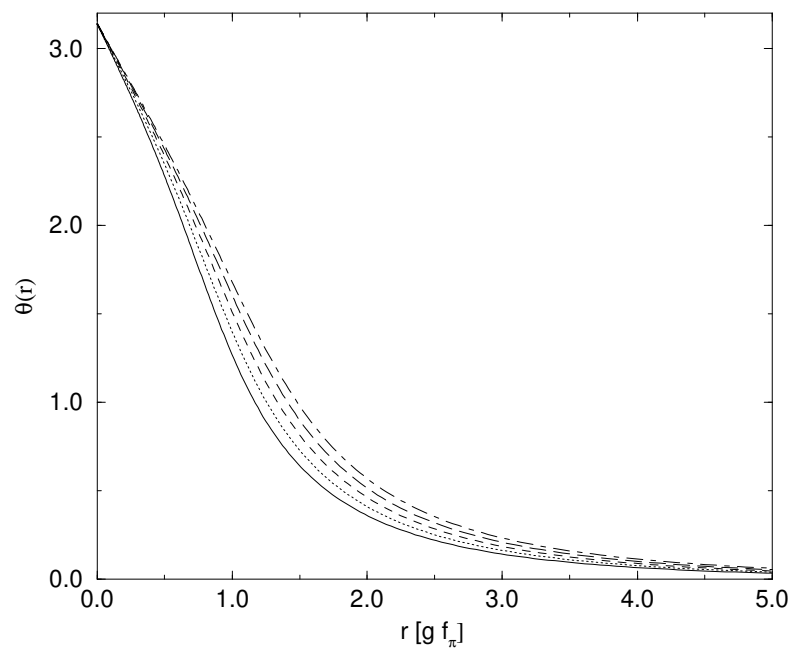


Fig. 5

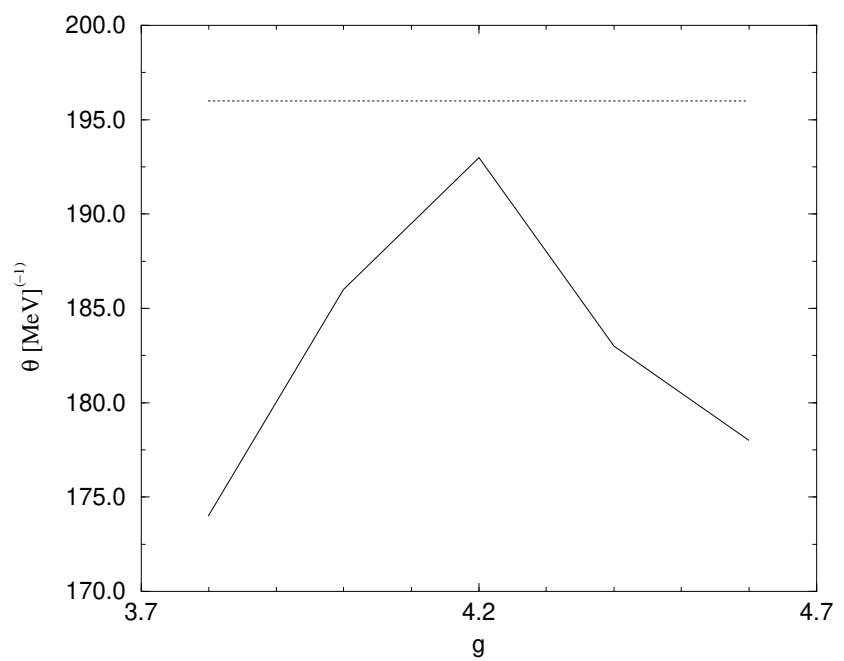


Fig. 6